

Magnesium-lithium-alloys - constitution and fabrication for use in batteries

M. SAHOO

PMRL/CANMET, Energy, Mines and Resources, 568 Booth Street, Ottawa, Canada K1A 0G1

J. T. N. ATKINSON

Department of Metallurgical Engineering, Queen's University, Kingston, Ontario, Canada K7L 3N6

Additions of just over 10 wt% lithium to magnesium cause its crystal structure to become cubic and render the alloy readily workable. The present work studies the preparation and fabrication of binary Mg-Li and ternary Mg-Li-Al alloys and makes a preliminary assessment of their suitability as anodes in primary battery systems. The preferred technique is induction melting in a silicon carbide crucible, followed by chill casting, under a protective argon atmosphere. Single-phase alloys, including those with lower lithium content, require intermediate annealing. These alloys have similar corrosion resistance to other magnesium-base alloys such as AZ31 and give consistently higher voltages and better discharge characteristics during battery studies.

1. Introduction

Magnesium and its alloys such as AZ31 (Mg-3Al-1Zn) and AZ61 (Mg-6Al-1Zn) have long been used as the anode in dry batteries. A typical electrolyte is magnesium perchlorate, with additions of soluble chromates to reduce wasteful corrosion of the anode.

The addition of lithium to magnesium is unique in that as little as 10.5 wt% can change the crystal structure of the resultant alloy from hexagonal α (magnesium) to cubic β (lithium). The single phase (β) alloys are relatively soft and, for a Mg-base alloy, uniquely ductile. The cold-forming troubles associated with hexagonal crystal structure of magnesium or its other alloys may thus be avoided. Addition of lithium to magnesium also decreases its density.

In view of the high cost of lithium the present study was restricted to alloys of lithium content up to about 13 wt%. The lower limit of lithium was set at about 6 wt% below which the hexagonal α structure predominates. In the range 6 to

10.5 wt% lithium, the Mg-Li alloys exist as a mixed crystal structure (α and β).

Despite the fact that Mg is divalent it may well appear to behave as a monovalent in the battery and show 50% anode efficiency. The addition of trivalent or tetravalent elements which would remain in solid solution may improve the efficiency. The various elements which would remain in solid solution with magnesium are shown in Fig. 1 [1]. Since Mg-12% Li alloys containing 1% Zr or In were found to possess poorer corrosion resistance in the battery electrolyte [2-4], the ternary alloy part of this paper deals principally with Al as a third element.

2. Experimental details

2.1. Melting and casting

The magnesium and lithium used to prepare the alloys had typical analyses as shown in Table I. It should be noted that a sodium content of $>0.1\%$ in the Mg-Li alloys causes intergranular cracking during rolling. High purity materials are

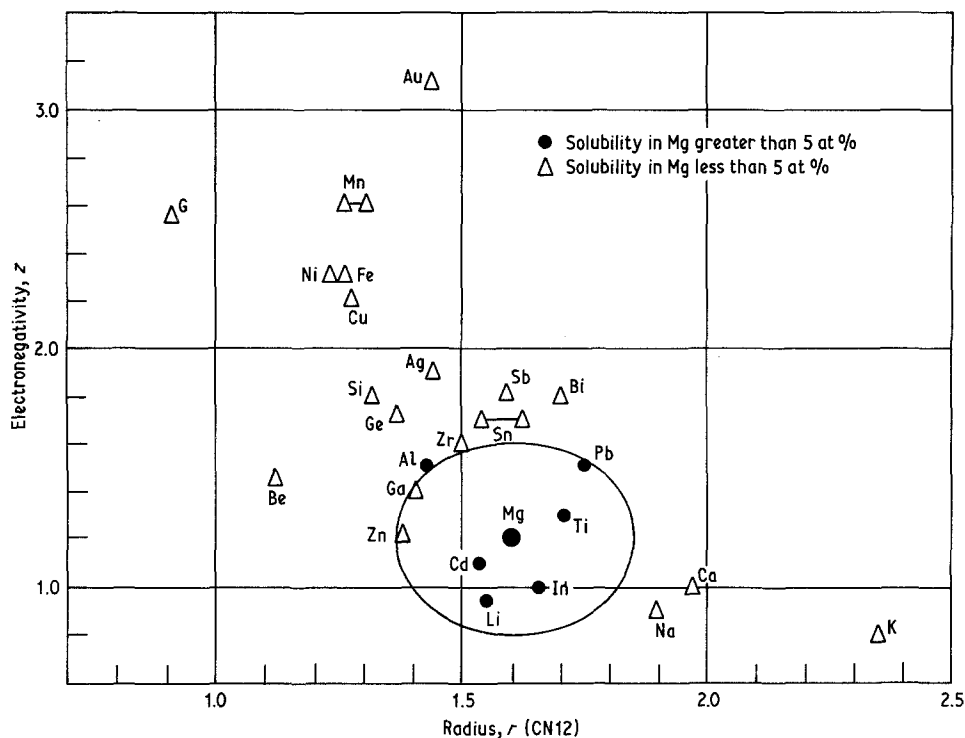


Figure 1 Chart of elements whose solubility in magnesium is known [1].

required, along with care to avoid Na pick-up in melting.

Mg-Li alloys can be melted satisfactorily under a flux cover or in an inert atmosphere [5]. It was found that the most successful method of melting and casting involved using the Balzers high-vacuum induction furnace under an argon atmosphere of 600 mm Hg. Preliminary trial runs by melting under argon in a low carbon steel crucible in a resistance-heated furnace had not given a homogeneous product in spite of vigorous stirring.

A variety of crucibles were used, with silicon carbide being most satisfactory. Steel might be acceptable for larger batches where iron pick-up from the crucible would be less significant. Before melting, magnesium and lithium were cleaned, respectively, in 5% nitric acid and in a solution of toluene containing 5% methanol.

TABLE I

Magnesium	Lithium
Mg 99.95%	Li 99.9%
Ni + Fe + Cu 0.005%	Na 0.035%
Si \leq 0.01%	K 0.0094%
Mn 0.01%	
Ca 0.002%	
Na, K approx. 100 ppm	

After induction melting the alloy was cast into a cold steel mould, still under argon, to obtain a casting of 28 mm \times 130 mm \times 240 mm. In order to minimize the chilling effect, the inside of the steel mould was coated with alumina. In addition, the steel mould was supported on refractory bricks inside the induction furnace.

2.2. Rolling

A two-high rolling mill with 150 mm diameter rolls was used for rolling. The rolls were not heated. In order to prevent adhesion, the rolls were coated with lubricating oil (Shell Tellus 29). Prior to rolling each alloy was homogenized at 300°C for 5 h and then skinned by milling to give a rectangular block free from visible casting defects.

2.3. Testing of the alloys

Most specimens for optical microscopy were cold mounted. After conventional grinding and polishing, β -phase alloys were etched with 2% HF solution, while 2% HNO₃ solution was preferred for the two-phase alloys.

The changes in mechanical properties with thermo-mechanical processing were monitored by Vickers hardness measurements carried out using 2.5 kg load. A Norelco X-ray diffractometer

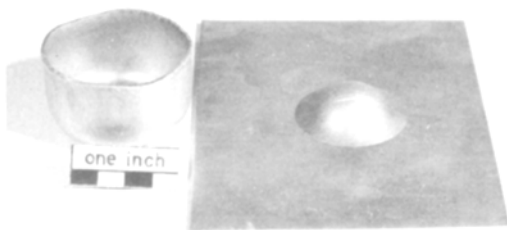


Figure 2 Typical Erichsen cup and deep-drawn cup for alloy I-4, cold-worked 90% and annealed at 200°C for 150 min.

was used to identify the structure of the Mg–Li alloys.

All tensile tests were performed at ambient temperatures ($\sim 25^\circ\text{C}$) using an Instron testing machine at a cross-head speed of $\sim 0.26\text{ mm min}^{-1}$. Specimens for tensile testing were 19.0 mm wide. Specimen elongation was measured over a gauge length of 51.0 mm.

Erichsen cupping tests and Swift flat bottom cup tests were carried out in the Tinius Olsen Ductomatic Sheet Metal Tester*. These tests provide a convenient way to evaluate the suitability of sheet metal for many forming and stamping operations. In the former test the sheet metal (76 mm \times 76 mm) is subjected to a ball indenter of 20 mm diameter. This action stretches the metal sample into the upper or drawing die, and is stopped when a crack occurs. The height of the cup is a measure of the ductility. The latter test was used to evaluate the formability and earing phenomena of the Mg–Li alloys. In this method a 55 or 60 mm diameter blank was deep drawn into a flat-bottomed cup like that shown in Fig. 2.

2.4. Static corrosion tests

To simulate the corrosion behaviour of the Mg–Li alloys in the battery electrolyte, a 2.5 N magnesium perchlorate solution containing 0.2% magnesium chromate was used. The rolled and annealed specimens, 0.8 mm \times 27 mm \times 40 mm, were cleaned in dilute HNO_3 , rinsed, weighed and immediately immersed in the perchlorate solution. After about 7 days at room temperature ($\sim 25^\circ\text{C}$), the specimens were washed in water and the corrosion product was removed by immersing for 3 min in a 20% chromic acid solution containing 1%

*Registered trade mark.

AgNO_3 . After drying, they were reweighed. The rate of corrosion was expressed as mdd (milligram/square decimeter/day). The test merely served as a screening operation to exclude unsatisfactory alloys from further testing.

2.5. Electrochemical studies

Cell discharge tests were conducted with one anode of the Mg–Li alloy in question positioned between two manganese dioxide-coated cathodes. The cell was discharged either into a constant external resistance, or at constant current drawn from an external power supply. The manganese dioxide cathodes were prepared on current collectors 38 mm wide by 50 mm high of expanded silver metal, each having a tab attached for electrical connection.

A dry mix was prepared consisting of either 87 parts by weight of manganese dioxide of a commercial battery grade and 13 parts by weight of 50% compression Shawinigan black; or 87 wt% manganese dioxide, 10 wt% Shawinigan black and 3 wt% pulverized barium chromate. The purpose of the barium chromate is to protect the anode against corrosion during long storage of batteries; this is unnecessary in the tests conducted here, as the test cells were discharged shortly after preparation. Nevertheless, the addition was made to see if the 87–10–3 mix gave results different from the 87–13 mix. No difference was in fact observed. The procedure for preparing the mix follows commercial battery practice closely.

In cathode preparation, a known weight of dry-blended cathode mix was spread, and levelled on an expanded silver grid so that the grid was located centrally in the mix. The composite was encased in a layer of No. 1 Whatman filter paper, moistened with a small amount of the electrolyte to be described below, and compressed at a sufficient pressure to allow for subsequent handling. The electrolyte was 1.5M magnesium perchlorate in water, inhibited with 0.3 wt% magnesium chromate.

The anode consisted of a sheet of the alloy being tested, approximately 35 mm wide by 50 mm high, to which had been spot-welded a wire at one corner for electrical contact. The spot weld was covered with silastic putty.

In most experiments, one anode and two cathodes were held together loosely, and the assembly placed in a small rectangular box and covered with electrolyte (about 30 ml). This provides a large

TABLE II Chemical composition, hardness and density of Mg–Li and Mg–Li–Al alloys

Melt no.	Crucible used	Melting process	Composition (wt%)			Density (g cm ⁻³)	Hardness (VHN)		
			Li	Fe	Al		As-cast	cold-rolled	Annealed*
19	Low-carbon steel	Resistance heating	11.8	0.0051	–	1.449	–	51.7	39.8
I-1	Low-carbon steel	Induction	12.2	0.01	–	1.454	38.9	53.7	39.7
I-2	Low-carbon steel	Induction	12.2	–	–	1.434	39.0	–	–
I-4	Low-carbon steel	Induction	12.2	–	–	1.434	39.2	–	–
I-7	Low-carbon steel	Induction	12.3	–	1.5	1.429	83.4	89.9	–
I-11	Graphite	Induction	11.8	0.0045	–	1.444	37.6	50.6	38.5
I-14	Graphite	Induction	11.8	0.01	–	1.445	35.1	49.4	–
I-17	Zirconia	Induction	9.5	0.0031	–	1.482	41.6	64.3	51.2, 41.4 [†]
I-21	Silicon carbide	Induction	12.5	0.0025	–	1.440	37.4	48.3	–
I-22	Silicon carbide	Induction	9.5	0.0035	–	1.490	38.3	63.4	–
I-25	Magnesia	Induction	11.5	0.0027	–	1.455	36.7	–	–
I-28	Silicon carbide	Induction	8.4	–	–	1.517	39.9	59.8	–
I-29	Silicon carbide	Induction	6.4	–	–	1.556	42.2	72.0	–
I-30	Silicon carbide	Induction	9.5	–	0.5	1.495	55.2	78.3	47.1

*150°C, 1 h.

†300°C, 1 h.

excess of electrolyte over that normally used in commercial “dry” cells and relatively easy access of the electrolyte to the interior of the cell.

In a few experiments the anode and cathode were compressed in a jig held in a vice so that they were totally enclosed, with a much smaller amount of electrolyte being added beforehand. These conditions more nearly simulate the liquid-starved environment of a normal dry cell.

3. Results and discussion

3.1. Compositions

The chemical compositions of a number of alloys determined by the Atomic Absorption (AA) method are shown in Table II. It is evident that when melting is carried out in the steel crucible in the induction furnace, an appreciable amount of iron is picked up.

A plot of density against wt % Li was then prepared in the range 0 to 16 % Li (Fig. 3). The lithium level of each new alloy was then readily obtained from a simple density measurement in acetone. Density was found to be insensitive to the amount of cold work, thermal treatment, or location in the casting. This indicates that induction melting produces homogeneous Mg–Li alloys.

3.2. Annealing behaviour

For the single-phase and two-phase alloys, recovery after cold work was completed below 50°C, whilst recrystallization took place at about 150°C. The presence of aluminium did not change the recrystallization temperature. In the case of

the single-phase (β) alloys recovery also took place at room temperature over an extended period of time.

3.3. Rolling characterization

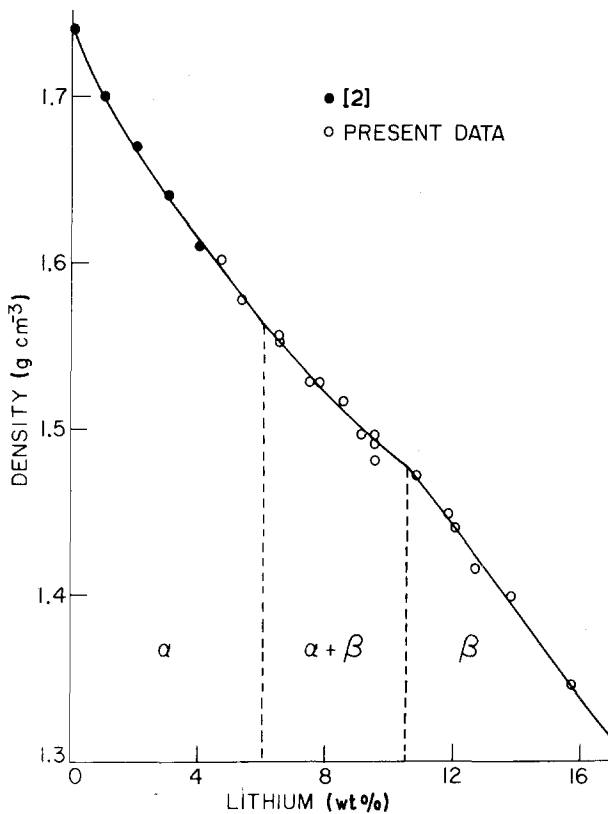
The single-phase alloys could be easily cold rolled by 97%. However, an interim annealing treatment of 3 h at 300°C was given after the first 50% cold working. After each annealing treatment, rolling was continued in the hot condition until the temperature dropped to room temperature.

Despite the presence of 19 vol % hcp α -phase in the bcc β -matrix, the rolling characteristics of the Mg–9.5% Li alloy was similar to that of the single-phase Mg–12% Li alloy. Thus it could be rolled to thin sheets by employing only one interim annealing treatment.

The Mg–8.5% Li alloy contains 38 vol % α -phase in the β -matrix. More work hardening could thus be expected in this alloy during cold rolling. When the alloy was subjected to a similar rolling procedure 0.8 mm thick sheets could be produced following 80 to 95% cold reductions. However, the rolled sheets contained numerous edge and surface cracks. Two more interim annealing treatments (300°C, 45 min each) were necessary for crack-free 0.8 mm thick sheets to be produced.

The Mg–7.5% Li alloy corresponds to the eutectic composition and contains about 50 vol % α -phase in the β -matrix. As expected, this alloy could not be easily cold rolled without producing a lot of edge and surface cracks. Thus several

Figure 3 Density of binary Mg–Li alloys at room temperature.



annealing steps were employed to produce 0.8 mm thick sheets. Although this alloy may not be of industrial significance because of the high cost of fabrication, it is suggested that for successful rolling the alloy be annealed at 300°C for 30 min after each 30% hot and cold reduction. A hypoeutectic 6.5% Li alloy could be successfully rolled with a similar schedule. It contained about 21 vol % cubic β -phase in the hexagonal α -matrix.

Mg–Li alloys containing 1 to 2% Al are typical precipitation-hardening alloys and it has been reported that precipitation can take place at room temperature following solution treatment [6, 7]. This is also evident from the hardness of the cast Mg–12% Li–1.5% Al alloy (Table II). Because of the precipitation of the second phases during air cooling following homogenization at 300°C for 5 h, the ductility decreases. As a result the Mg–12% Li–1.5% Al alloy could not be cold rolled and cracks appeared after only 10% cold working. In order to produce 0.8 mm thick sheets it was necessary to hot roll 15 to 20% after each annealing treatment at 300°C. This type of rolling and annealing cycle was repeated until the thickness was reduced to about 2.5 mm. After such hot-

breaking down, the alloy could then be cold rolled to 0.8 mm thick sheets.

With a view to reducing the volume fraction of the precipitating phase, the aluminium level was limited to 0.5% in the Mg–9.5% Li alloy. This homogenized alloy could be cold rolled 50% when a few edge cracks appeared. For the production of 0.8 mm thick sheets this alloy requires only three interim annealing treatments at 300°C. Thus the rolling characterization of the Mg–9.5% Li–0.5% Al alloy are similar to those of the Mg–8.5% Li alloy.

3.4. Microstructure

Optical micrographs corresponding to the cold-rolled and annealed condition for the two-phase Mg–Li alloys are shown in Fig. 4a, b and c for different lithium contents. Thermomechanical processing of these two-phase alloys has produced a fine grain microstructure. By contrast, the grain size of the single-phase Mg–12% alloys was of the order of 1 mm for the cold rolled and annealed (300°C, 1 h) conditions.

Microstructures of the precipitation-hardening Mg–Li–Al alloys have already been described in the literature [6, 7].

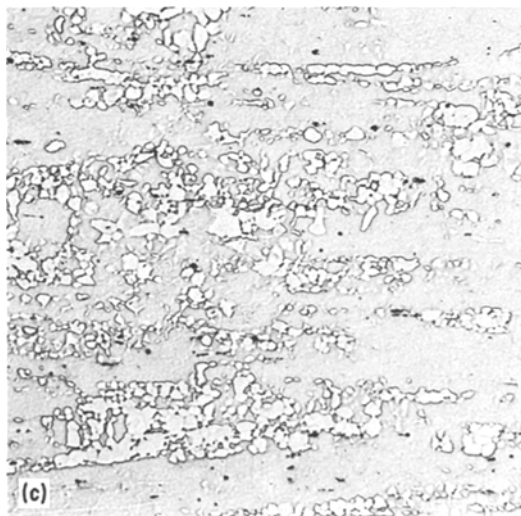


Figure 4 Optical micrographs of two-phase Mg–Li alloys. (a) Mg–5.5% Li (I-29); hot-rolled and then cold-rolled 40% to $t = 0.9$ mm followed by annealing at 300°C for 1 h. (b) Mg–7.5% Li alloy (I-12); hot- and cold-rolled to $t = 1.1$ mm and then annealed at 300°C for 1 h. (c) Mg–9.5% Li alloy (I-17), cold-rolled 90% to $t = 0.8$ mm and then annealed at 300°C for 1 h. ($\times 100$).

3.5. Tensile properties

Limited tensile tests were conducted on specimens sheared at various angles to the rolling direction. The results are summarized in Table III. It is evident that the yield and ultimate tensile strengths are independent of the angle between the tensile axis and the rolling direction, and indicate that a pronounced texture is not developed. The elongation to fracture for the annealed alloys exceeded 60% except for those sheared at 90° to the rolling direction.

3.6. Erichsen cupping tests

The results of the Erichsen cupping tests are shown in Table IV. The cup height, which is a measure of the ductility of the alloy, compares favourably with figures generally quoted for alu-

minium [8]. The best results were obtained with the recrystallized sheets. The type of annealing treatment did not appreciably alter the Erichsen values. A typical Erichsen cup is shown in Fig. 2. It may be noted from Table IV that the cup height is a function of the thickness of the sheet. However, when the thickness was kept constant the cup height was found to diminish with decreases in the lithium level in the two-phase alloys and the Mg–6.5% Li alloy showed the minimum ductility in the annealed condition. Although this was not confirmed by tensile tests, such decreases in ductility are to be expected.

3.7. Deep-drawing characteristics

The deep-drawing characteristics are summarized in Table V. Although the drawability of the alloys has not been evaluated in detail, the limited test results indicate that the annealed sheets showed less than 5% earing with the exception of the Mg–9.5% Li alloy. Thus in the manufacture of anode cups of various configurations, directionality is not likely to cause any problem. The presence of 0.5% Al in the Mg–9.5% Li alloy did not adversely affect the deep-drawing characteristics. It is important to note that AZ31 and AZ61 alloys could not be deep drawn in spite of several variations in the draw ratio.

TABLE III Room temperature tensile properties of induction-melted Mg-12% Li alloys (I-2)

Specimen condition	θ^* (deg)	0.2% offset yield strength (N mm ⁻²)	Ultimate tensile strength (N mm ⁻²)	Uniform elongated [†] (%)	Total elongation (%)
Cold-rolled 90%	0	39.6	89.4	6.0	39.0
	45	40.4	85.6	3.3	85.0
	90	49.8	96.1	3.6	15.5
Cold-worked 90% and annealed at 150° C for 60 min	0	51.3	78.2	1.6	64.0
	45	56.8	77.2	1.5	75.0
	90	49.7	79.9	1.7	28.0
Cold-worked 90% and annealed at 200° C for 90 min	0	69.9	80.6	1.5	64.0
Cold-worked 90% and annealed at 200° C for 150 min	45	65.4	78.5	2.2	> 70%

* θ -angle between rolling direction and the tensile axis.

[†]Permanent elongation before the onset of necking.

TABLE IV Erichsen cupping values for Mg-Li and Mg-Li-Al alloys. Test conditions: load rate 12.7 mm min⁻¹ (0.5 in. min⁻¹), diameter of ball 20 mm, diameter of holder 27 mm; the ball was lubricated with vaseline before each test.

Melt no.	Crucible used	Composition (wt %)	Specimen condition	Thickness (mm)	Cup height* (mm)
I-2	Low-carbon steel	12.2 Li	Cold-worked 90%	0.965	4.9
			Cold-worked 90% and annealed at 150° C for 120 min	0.690	7.6
			Cold-worked 90% and annealed at 200° C for 150 min	1.092	7.6
			Cold-worked 90% and annealed at 300° C for 180 min	1.092	8.0
I-4	Low-carbon steel	12.2 Li	Cold-worked 90%	1.02	5.8
			Cold-worked 90% and annealed at 150° C for 60 min	1.02	8.0
			Cold-worked 90% and annealed at 200° C for 150 min	1.00	8.1
I-11	Graphite	11.8 Li	Cold-worked 90% and annealed at 150° C for 60 min	0.94	7.6
I-17	Zirconia	9.5 Li	Cold-worked 90% and annealed at 300° C for 60 min	0.821	7.7
I-28	Silicon carbide	8.4 Li	Cold-worked 55% and annealed at 300° C for 60 min	0.81	6.1
I-29	Silicon carbide	6.4 Li	Cold-worked 40% and annealed at 300° C for 60 min	0.81	4.8
I-30	Silicon carbide	9.5 Li and 0.5 Al	Rolled and annealed at 300° C for 5 h	0.66	6.4

*In each case orientation of fracture was along the rolling direction.

TABLE V Drawability of Mg–Li alloys. Test conditions: blank was lubricated with vaseline on both faces; load rate of 12.7 mm min⁻¹ (0.5 in. min⁻¹); Room temperature.

Melt no.	Crucible used	Composition (wt %)	Specimen condition	Thickness (mm)	Blank size (mm)	Die diameter (mm)	Draw ratio	% Earing*
I-2	Low-carbon steel	12.2 Li	Cold-worked 90% and annealed at 150° C for 60 min	1.092	60	36.45	1.703	1.9 (3)
I-4	Low-carbon steel	12.2 Li	Cold-worked 90% and annealed at 200° C for 150 min	1.02	60	36.63	1.710	4.7 (4)
I-17	Zirconia	9.5 Li	Cold-worked 90% and annealed at 300° C for 60 min	0.85	60	35.76	1.70	14.2 (3)
				0.86	55	35.76	1.59	10.2 (6)
I-28	Silicon carbide	8.4 Li	Cold-worked 55% and annealed at	0.79	60	35.76	1.70	4.5 (5)
				0.86	55	35.76	1.59	3.3 (3)
I-29	Silicon carbide	6.4 Li	Cold-worked 40% and annealed at 300° C for 60 min	0.86	60	35.76	1.70	failed (3)
				0.86	55	35.76	1.59	1.9 (3)
				0.821	55	35.76	1.59	1.1 (3)
				0.81	60	35.76	1.70	failed (1)
				0.81	60	35.76	1.70	2.2 (1)
I-11	Graphite	11.8 Li	Cold-worked 90% and annealed at 150° C for 60 min	0.914	60	36.45	1.703	3.3 (3)
I-30	Silicon carbide	9.5 Li 0.5 Al	Cold-worked 55% and annealed at 300° C for 60 min	0.76	55	35.76	1.59	8.2 (2)

* Average value. The number in parenthesis refers to the number of determinations.

3.8. Corrosion behaviour

The results of the static corrosion tests in the perchlorate solution are given in Table VI along with comparison tests on AZ31 alloy. Preliminary tests showed that the rate of corrosion was independent of the thermomechanical condition of the alloy. Since heavily cold-worked alloys are in any case likely to recover at room temperature it was decided to conduct future corrosion tests on annealed samples.

Table VI shows that the corrosion resistance of the Mg–12% Li alloys is independent of the crucible material and is similar to that of the AZ31 alloy. As the Li content of the alloys increases, the corrosion resistance appears to decrease. Addition of aluminium to both the single- and two-phase alloys seemed to enhance the corrosion resistance.

3.9. Electrochemical behaviour

A direct comparison of two discharges conducted under identical conditions (i.e. flooded cell, 5.73 Ω

external resistance and 4 g dry mix per cathode) is shown in Fig. 5 for commercial alloy AZ31 and single-phase Mg–12% Li alloy. It shows that the Mg–Li alloy voltage is higher by almost 0.2 V during most of the discharge. A similar trend was observed for discharges through a similar resistance under liquid starved conditions as shown in Fig. 6.

A voltage of 1.6 V and an external resistance of 5.73 Ω correspond to a current of 280 mA. The current density at the anode (both sides) is 8.7 mA cm⁻².

In another experiment, as shown in Fig. 7, the same alloys were used as power supplies in the flooded cell configuration. Starting at open circuit, each was maintained for 7 min at each current setting shown from 0 to 17 mA cm⁻² and return, with the voltage being recorded at the end of each time interval. The voltage advantage of the Mg–Li alloy over the AZ31 is again seen. The hysteresis loop is larger for AZ31 than for the Mg–Li alloy. In

TABLE VI Static corrosion data for Mg–Li and Mg–Li–Al alloys in perchlorate solutions

Melt no.	Crucible material	Composition	Specimen condition		Corrosion rate (mdd)
			% cold-worked	Annealing treatment	
I-4	Low-carbon steel	12.2% Li	90	250° C, 1 h 300° C, 1 h	33.3 5.4
I-7	Low-carbon steel	12.3% Li and 1.5% Al	70	250° C, 1 h 300° C, 1 h	9.0 3.8
I-14	Graphite	11.8 Li	90	250° C, 1 h 300° C, 1 h	34.8 5.7
I-17	Zirconia	9.5% Li	88	250° C, 1 h 300° C, 1 h	15.3 16.5
I-21	Silicon carbide	12.5% LI	90	250° C, 1 h 300° C, 1 h	32.6 24.3
I-22	Silicon carbide	9.5% Li	90	250° C, 1 h 300° C, 1 h	16.3 3.1
I-25	Magnesia	12% Li	90	250° C, 1 h 300° C, 1 h	20.0 14.4
I-28	Silicon carbide	8.4% Li	55	250° C, 1 h 300° C, 1 h	12.8 8.3
I-29	Silicon carbide	6.4% LI	40	250° C, 1 h 300° C, 1 h	9.2 14.0
I-30	Silicon carbide	9.5% Li 0.5% Al	80	250° C, 1 h 300° C, 1 h	6.8 4.0
AZ31	—	—	—	As-received 300° C, 1 h	16.5 8.3

addition the Mg–Li alloy nearly regains its original open circuit voltage at the end of the cycle.

Similar studies were conducted on two-phase Mg–Li alloys and ternary Mg–Li alloys containing Al. The main finding was that in all circumstances the Mg–Li alloys gave consistently higher voltages than AZ31, and the voltage–time curves were flatter, i.e. there was less voltage “drop” during discharge. The effect is that cells using the Mg–Li alloys consistently deliver some 15% more power than AZ31 to a final cut-off voltage of 1.98 V. This is a normal criterion for practical batteries.

4. Conclusions

Although Mg–Li alloys can be easily melted in crucibles made of low-carbon steel, graphite and refractory materials such as zirconia, magnesia or silicon carbide, the steel crucibles may be preferred in industrial practice to economize the process, unless the electrochemical properties of the

alloy are adversely affected. The low recrystallization temperature of the alloys allows a simple drying oven to be used for annealing treatments.

An examination of the static corrosion studies and the electrochemical behaviour of the alloys tends to indicate that, in the range 6.5 to 12% Li, Mg–Li alloys can be successfully used as anodes in dry batteries to replace the conventional AZ31 alloy. The rolling and deep-drawing characterization show that it is cheaper to fabricate the Mg–Li anode cups. Although lithium is costly, it is anticipated that if these alloys are mass produced, the cost of lithium will eventually come down. It was also found that the use of smaller amounts of lithium as in Mg–6.5% Li and Mg–8.5% Li alloys retained most of the electrochemical advantages and may off-set the additional cost involved in fabrication relative to Mg–12% Li.

Although small amounts of aluminium may be added to enhance the static corrosion resistance,

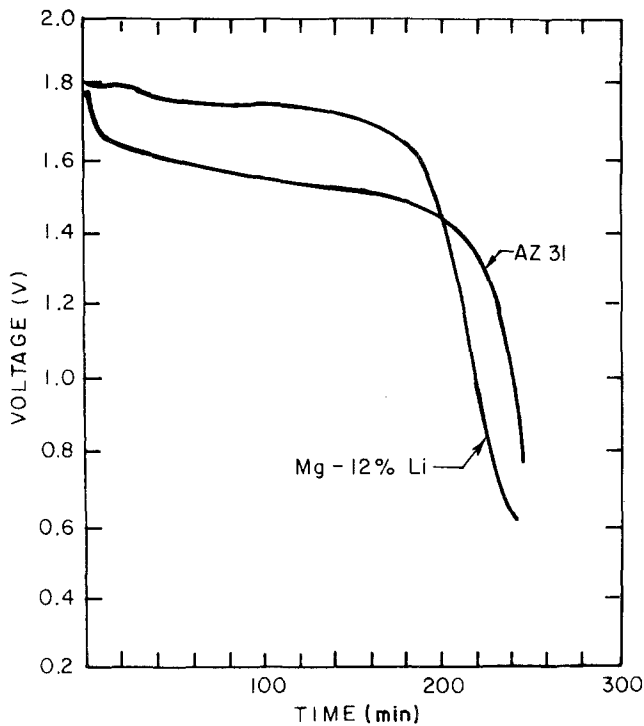


Figure 5 Discharge curves (flooded condition).

additional thermomechanical steps may be required to fabricate the alloys. Electrochemical properties are substantially unchanged.

Acknowledgements

The financial assistance of the Department of Supply and Services is gratefully acknowledged.

We are indebted to Drs J. R. Coleman and J. G. Donaldson, Defence Research Establishment, Shirley Bay, Ontario, Canada, for conducting the battery studies and to Mr R. Lidstone, Alcan Research Laboratory, Kingston, Ontario, for the provision of the Tinius Olsen Ductomatic Sheet Metal Tests. Thanks are also extended to Messrs Ajit

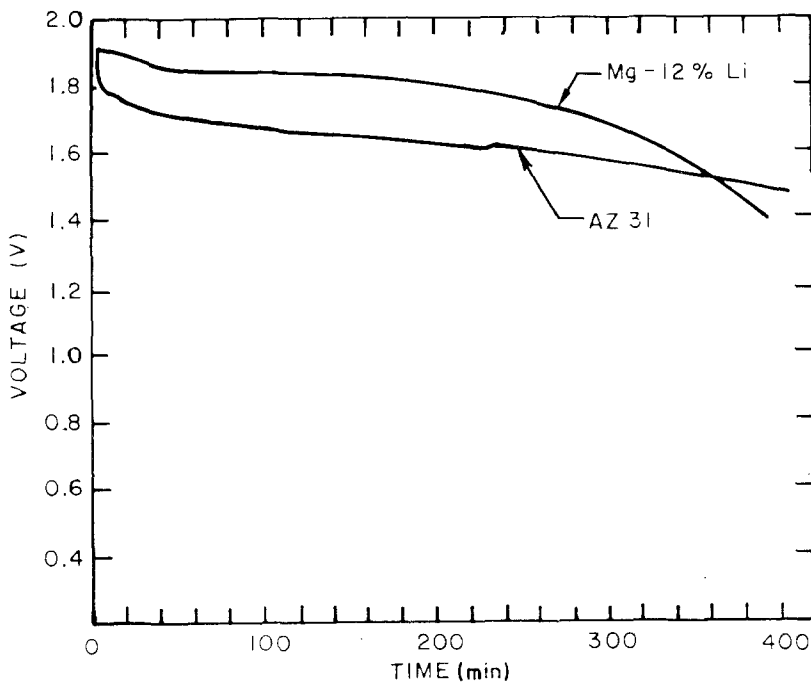


Figure 6 Discharge curves (starved condition).

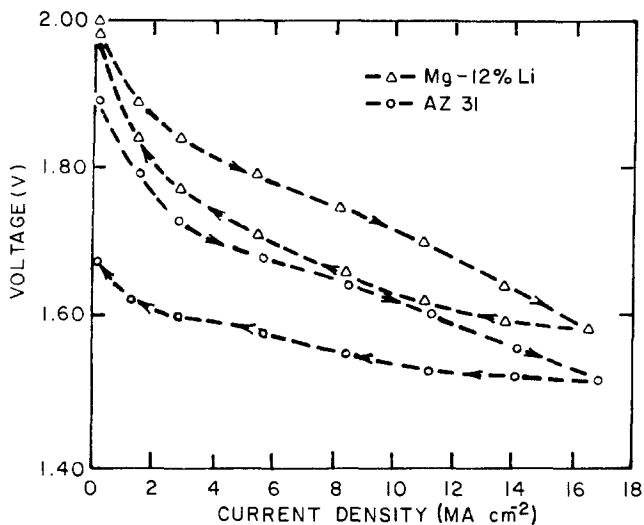


Figure 7 Discharge cycling tests (flooded condition).

Sarma and T. F. Lee for electing final year projects which contribute to the study by determining mechanical characteristics of the Mg-12% Li alloys.

References

1. L. S. DARKEN and R. W. GURRY, "Physical Chemistry of Metals" (McGraw Hill, New York, 1953) p. 87.
2. M. SAHOO, T. F. LEE and J. T. N. ATKINSON, "The Production of Mg-Li-Alloys", Progress Report from 1 April to 30 June (1977). Department of Supply and Services Research Project 12ST.CD1410525. Department of Metallurgical Engineering, Queen's University Kingston, Ontario.
3. M. SAHOO and J. T. N. ATKINSON, *ibid.*, Progress Report from 1 July to 30 September (1977).
4. I. C. PLATT and J. T. N. ATKINSON, *ibid.*, Progress Report from 1 January to 31 March (1978).
5. E. H. ADOLF BECK, "The Technology of Magnesium and its Alloys" (Hughes, London, 1940) p. 314.
6. W. R. D. JONES, *J. Inst. Met.* **84** (1955-56) 364.
7. H. M. SKELLY, "A survey of Literature on Mg-Li Alloys", Report No. K-TM-273-55-37. Aluminum Laboratories Ltd (1956).
8. R. LIDSTONE, Alcan Research Laboratory, Kingston, Ontario. private communication (1977).

Received 31 January
and accepted 17 May 1982